A Modified Aston-Type Mass Spectrometer and Some Preliminary Results

D. D. TAYLOR, *Norman Bridge Laboratory of Physics, California Institute of Technology*

(Received January 7, 1935)

A modified Aston-type mass spectrometer is described, in which ionization is produced by controlled electron bombardment. The electric field used is radial, and the shape of the magnetic pole faces was calculated to give the necessary velocity focusing. A special type of filament assembly is employed to minimize the energy spread of the emitted electrons. An amplifier circuit is described using a Western Electric D-96475 tube which gives high sensitivity combined with good stability. A new device is described for giving a continuous indication proportional to the square of the magnetic field. Some preliminary results are included on the ionization of N_2, CO, NH_3, N_2H_4.

IN order to obtain increased resolving power for the study of positive ions resulting from controlled electron bombardment, a modified Aston-type mass spectrometer has been constructed and some preliminary results will be given. The general arrangement is shown in Fig. 1. The gas to be investigated is admitted at G into a capillary tube. The gas is released from the capillary at about the center of the filament assembly F where it is bombarded by electrons accelerated radially inward. The resulting ions are then accelerated by a 1500-volt potential applied between F and the anticathode A. A is grounded through a microammeter to permit measurement of the positive ion current incident on it, which is used as an indication of the total current through the mass spectrometer. The collimator consists of two slits, C, 40 cm apart and each 2.5 mm$\times$0.1 mm. The collimated beam next passes through the electric deflecting field E whose plates are equiangular sectors of coaxial cylinders, and in this field the beam is spread out into an energy spectrum. This divergent beam next enters the magnetic field M whose leading and trailing edges were calculated to focus all particles of a given value of e/m on the focal slit S, and any desired value of e/m can be focused by suitable adjustment of the magnetic field strength. The leading and trailing edges of M are slightly concave but no attempt has been made to indicate their true shape for the drawing is too small.

With the exception of necessary electrical insulation the apparatus is constructed of metal. The magnetic circuit is made of Rema dead soft electric furnace charcoal iron. The remainder of the apparatus is of brass, with gold slit jaws and gold plated deflecting plates. The plug of the large ground joint carrying the filament assembly is of Pyrex ground into a steel sleeve.

The path of a charged particle in the radial electric field was kindly obtained by Mr. G. C. Munro of this laboratory. Neglecting edge effects the field between the two plates is an inverse first power field. All the rays are assumed to be parallel and to enter the field at the same point, on the leading edge midway between the plates. It is required to find the emergent paths and velocities for the velocity determines the radius of curvature in the magnetic field and the emergent path determines the point of incidence in the field. The point of emergence of the ray on the trailing edge of the electric field, the emergent velocity, and the angle between the emergent ray and a reference ray were each determined in terms of one of three convergent infinite series in a parameter, $\kappa=\phi_0/2E \ln(\rho_2/\rho_1)$. ϕ_0 is the voltage applied between the electric field plates of radius ρ_2 and ρ_1, and E is the energy of the particle in electron volts. If the center of curvature of the plates is taken as the origin, a circle of radius α about this point passes through the point of incidence of the rays and the radius to the point of emergence of any ray is $\rho=u\alpha$. u is described by $u=1+(1-\kappa)f(\kappa)$.

The tangent of the angle between the emergent ray and the reference ray is $(1-\kappa)F(\kappa)$. The relation between the emergent velocity V and the incident velocity v is $V^2=v^2[1-\kappa(1-\kappa)\phi(\kappa)]$.

A range of κ from 0.7 to 1.3 covered the entire usable part of the field but the calculations

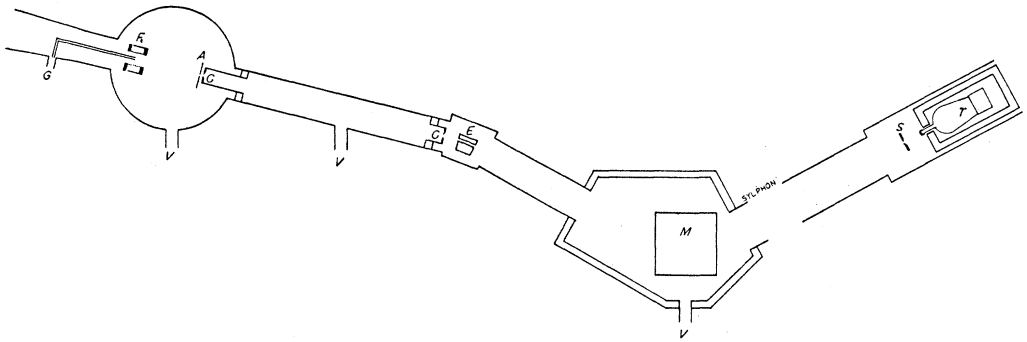

FIG. 1. Diagram of mass spectrometer. *G*, gas inlet to capillary; *F*, filament assembly—see Fig. 2; *A*, graphite anticathode; *C*, collimator slits; *E*, electric deflecting field; *M*, magnetic deflecting field; *S*, focal slit; *T*, Western Electric Co. D–96475 tube; *V*, vacuum pumping connections.

were extended from $\kappa = 0.5$ to 1.5. Since the analysis of the electric field disclosed no analytic expression for the characteristics of the beam after traversing the electric field, the only available method of determining the proper shape of the magnetic field lay in assigning appropriate values to the parameter κ and then determining radius of curvature and point of incidence on the magnetic field for a sufficient number of rays. It was found that the calculation could be greatly simplified by introducing the further restriction on the magnetic field that it be symmetrical with respect to the bisector of the angle between the incident and emergent median rays. A total of fifty-five points was calculated on the leading edge of the magnetic field and then by means of a Schwartz transformation the edge effect was investigated and the points were corrected accordingly. The results of the edge effect calculation show that to a reasonable approximation the line integral of the magnetic field along the path of a particle is the same as if the uniform field were taken to extend beyond the edge a distance equal to eight-sevenths of the air gap.

An attempt was made to approximate the curve by means of an ellipse which could be generated on a milling machine, but no conic section gave a satisfactory fit.

The half-width of the iron at the bottom of the field is 1.789 inches, the minimum half-width is 1.768 at 1.600 inches above the bottom, and the half-width is 1.808 inches at a point 3.0 inches from the bottom, above which no rays enter.

A sylphon is introduced between the magnetic field and the focal slit to permit radial and tangential motion of the focal slit for adjustment of focus.

Unfortunately the theoretical work of R. Herzog[1] was not available when this apparatus was designed but it has since been applied. The electric deflecting field has a radius of curvature for the median ray of 12 cm and is equivalent to a cylindrical lens of 24.5 cm focal length plus a prism. The magnetic field has a radius of curvature of 10 cm for the median ray and is equivalent to a cylindrical lens of 11.9 cm focal length plus a prism. In both fields the intersection of the principal planes coincides with the intersection of the median rays. The first collimator slit has an inverted image 33.3 cm in front of the focal slit *S*, and the image of the second collimator slit is 23.8 cm in front of *S*. The width of image observed at *S* is consistent with that calculated from the positions and dimensions of their optically determined images.

Vacuum pump connections are provided at the three points marked *V*.

The filament assembly is shown in more detail in Fig. 2, and has proven quite satisfactory in most respects. The entire body is made of Acheson graphite and consists of two disks and a short cylinder attached to one of them. Eight helical tungsten filaments *F* are arranged as shown and no electrical connection to them is required other than a sliding fit in the holes drilled in the graphite. The grid *G* is

[1] R. Herzog, Zeits. f. Physik **89**, 457 (1934).

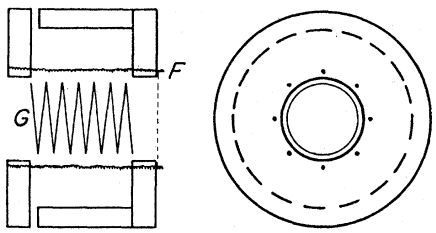

FIG. 2. Filament assembly diagram. *G*, helix of tungsten wire for grid; *F*, helical tungsten filaments.

also helical and is so proportioned that it withstands a potential drop equal to and in the same direction as that in the filaments, thus largely eliminating the variation in electron energy due to the filament drop. This also results in an axial field tending to draw the positive ions out of the filament assembly where they can be affected by the larger field applied between *F* and *A*. The chief disadvantage of this arrangement is the penetration of the larger field into the filament assembly so that as yet no check on ionization potentials is possible.

The amplifier circuit employed, as shown in Fig. 3, is notable chiefly for its simplicity for it has not been found necessary to modify the circuit for individual tube differences. The resistance values given were calculated only to give the recommended potentials and the behavior of the circuit has been most satisfactory from the start. The zero drift is consistently less than 2 cm per hour with a sensitivity of 10^{-17} amp./mm, and random fluctuation of 3–4 mm, which compares favorably with the various compensated circuits published up to this time. Two factors contribute to this stability. The first is the use of large batteries, 240 amp. hr. capacity, so that the voltage drift is negligible. The second is the careful shielding against thermal disturbances in addition to the necessary careful electrical shielding. All of the resistances in the circuit, excepting only the grid resistance of 10^{12} ohms, are immersed in transformer oil which effectively prevents temperature fluctuations. The number of variable contacts is reduced by soldering all possible contacts, leaving only those needed for adjusting filament current and galvanometer zero. Some trouble was caused by poor insulation resistance in the leads from the control box to the tube

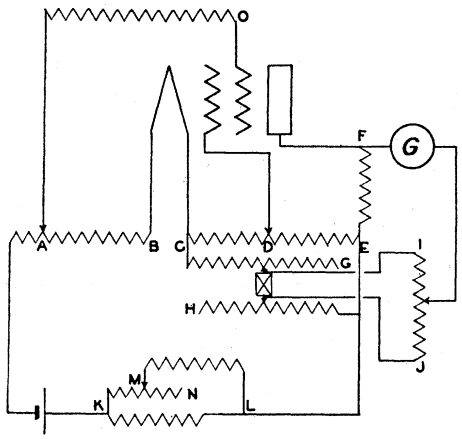

FIG. 3. Circuit diagram. Resistance $AO=1.3\times10^{12}$; $AB=11.1$; $CD=12.25$; $DE=8.65$; $EF=25{,}000$; $CG=200$; $EH=200$ (dual); $IJ=2$; $KL=10$; $KN=200$; $LM=40$. Battery—12v, 240 amp. hours. Galvanometer Type R, sens. about 10^{-9} amp./mm.

but the substitution of lead covered telephone cable eliminated the leakage. (This cable can be obtained having a guaranteed minimum insulation resistance of 500 megohm miles.)

The tube employed is the Western Electric D–96475 and it is a very definite improvement over the similar tubes previously available. It is mounted, as shown at *T* in Fig. 1, directly in the high vacuum of the mass spectrometer, and is protected by a half-inch of Rema iron from the stray field of the magnet *M*. In this construction the tubulation for the control grid lead is most convenient. The high resistance is mounted on the grid cap along with a small collecting electrode immediately behind the focal slit.

An auxiliary device is employed which gives a continuous indication of magnetic field strength. This takes the form of a plate of diamagnetic material, in this case Acheson graphite, suspended in the upper part of the magnetic field from a torsion balance. The force exerted on the plate tending to push it out of the field is proportional to the square of the field strength, and thus directly proportional to the m/e value of the ion brought to focus by that field strength. A mirror is mounted on the torsion balance for optical reading and the molecular weights so obtained readily fall within one percent of the true values, which is amply close for identification.

An attempt to utilize piano steel wire for the torsion fiber resulted in excessive zero shift due to elastic hysteresis, but the use of pure tungsten wire, even without annealing, has made this effect inappreciable.

The taking of observations involves plotting simultaneously the magnetic balance deflection and the positive ion current to the amplifier against an independent parameter, which for convenience is taken as the resistance inserted in the magnet circuit. This resistance is continuously variable from its maximum value of twenty-two ohms to about one-tenth ohm.

The results are presented in tabular form with one specimen curve from each substance to give a better idea of the form of the results obtained. To facilitate comparisons the peak heights are all given as percentages of the height of the primary peak. The column headed μa gives the positive ion current received on the anticathode, the next column shows the electron current received on the grid, and the volts column shows the voltage impressed between the filament and the grid. However, because of interpenetration of the accelerating field for the ion, this is in all cases higher than the true value of the energy possessed by the bombarding electrons. The next column shows the true height in cm of the primary peak, one cm representing a positive ion current to the collector of approximately 10^{-16} amp. The pressure in the ionizing chamber was of the order of 10^{-4} mm.

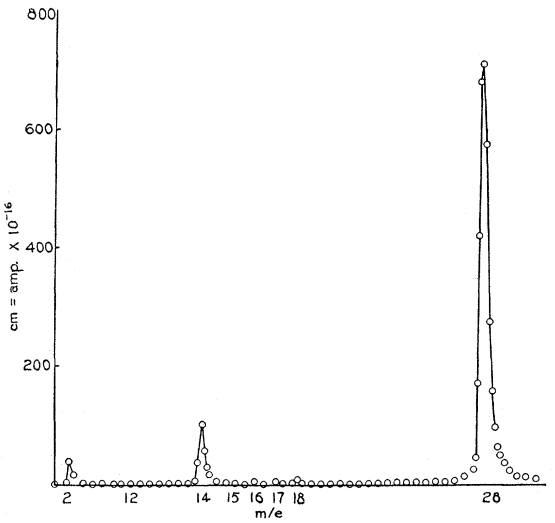

FIG. 4. Run No. 1. Nitrogen. 118 volt electrons. Height of N_2 peak = 705 cm.

NITROGEN

The nitrogen used was prepared by the thermal decomposition of sodium azide NaN_3 which is a very convenient source of pure nitrogen. Nitrogen within the voltage range considered yields predominantly molecular ions and shows satisfactory agreement with previous work on this substance. Although the source of the nitrogen precludes any possibility of its contamination with water vapor, nevertheless the walls of the apparatus apparently yield some water vapor and some organic vapor may be present from stopcock grease to account for the hydrogen found. The carbon peak is satisfactorily accounted for in the use of a graphite mounting for the filaments. No satisfactory explanation has been found for the two peaks appearing consistently at 39 and 41. The NH_3 and NH_4 peaks are certainly enhanced somewhat by OH and H_2O but no separation of the two was possible. The peak corresponding to atomic hydrogen ion was beyond the range of the apparatus so was necessarily omitted. Run No. 1 is shown as Fig. 4. (See Table I.)

TABLE I. *Ion intensities observed for nitrogen bombarded with electrons of various energies. Intensities calculated to basis* $N_2^+ = 100$. *μa = positive ion current incident on anticathode; ma = electron current incident on grid.*

Run	μa	ma	Volts	True N_2	H_2	C	N	NH	NH_2	NH_3	NH_4	CN	N_2	39	41
1	12	3	118	705	5.5	0.31	14	0.43	0.57	0.50	1.0	0.17	100	0.17	0.26
2	8	2	100	270	8.9	.56	18	.56	.74	.67	1.1	.37	100	.37	.74
3	11	3	80	110	8.6	2.7	29	.45	1.8	1.8	3.6	—	100	—	1.8
4	9	3	60	86	7.0	1.7	17	.46	1.2	1.2	2.1	—	100	—	—
5	5	7	40	56	13.	—	2.1	1.1	.9	2.0	5.4	—	100	—	1.1

TABLE II. *Ion intensities observed for carbon monoxide bombarded with electrons of various energies. Intensities calculated to basis $CO^+ = 100$.*

Run	μa	ma	Volts	True CO	H_2	C	CH	CH_2	CH_3	O	OH	H_2O	CO	39	41	CO_2
6	9	4	120	2075	15	1.7	0.05	0.38	0.29	0.77	0.39	1.2	100	0.10	0.14	0.63
7	12	5	120	1175	X	3.6	.04	.43	.38	1.3	.47	1.5	100	.17	.17	.60
8	25	12	120	430	X	19	.46	1.2	.58	5.8	.93	2.3	100	.35	.58	.93
9	50	26	120	14	X	370	7.0	18	7.0	160	—	—	100	—	—	—
10	20	12	120	1560	4.5	5.1	.13	.32	.22	1.2	.38	1.7	100	—	.13	.06
11	11	1.5	120	130	4.2	18	—	—	.6	2.3	3.8	20	100	—	.77	.54
12	8	3	100	365	6.8	9.8	—	.27	.02	3.2	.6	2.1	100	.55	.44	.41
13	11.5	18	80	29	52	21	—	—	—	14	3.5	6.9	100	2.8	—	—
14	9	5	80	125	4.4	19	.8	.56	.48	6.4	—	1.6	100	—	—	—
15	10	6	60	60	5.3	15	—	—	—	3.3	—	2.5	100	—	—	—
16	5	10	40	40	3.7	5	—	—	—	2	1.5	2.5	100	—	—	—

X = not covered in run. — = not found.

TABLE III. *Ion intensities observed for ammonia bombarded with electrons of various energies. Intensities calculated to basis $NH_3^+ = 100$.*

Run	μa	ma	Volts	True NH_3	H_2	C	N	NH	NH_2	NH_3	NH_4	N_2
17	10	0.1	117	18	14	33	78	8.3	86	100	139	680
18	20	2.5	117	7	43	36	190	21	130	100	71	400
19	9	2.5	114	17.5	31	7.1	7	10	104	100	74	40
20	19	8.5	110	21	76	16	12	12	107	100	100	79
21	30	11	110	17	47	7.3	13	13	130	100	12	35
22	9	.5	97	15	13	33	90	11	93	100	103	640
23	7	0.1	81	9.7	7.2	26	103	10.3	88	100	90	850
24	9	3	60	5.7	70	13	17	20	160	100	26	53
25	9	2	60	3.3	75	45	120	—	100	100	100	710
26	8.5	3.5	39	3.1	19	—	—	—	105	100	32	48
27	7.5	7.5	40	1.7	60	60	—	—	60	100	94	590

CARBON MONOXIDE

The carbon monoxide used was prepared by the dehydration with sulphuric acid of formic acid.

An interesting and unexplained effect is shown in runs 7, 8 and 9 which were made consecutively with everything unchanged except the electron current and correspondingly the positive ion current to the anticathode. It seems strange that a fourfold increase in the positive ion current should result in a decrease of the primary peak height to scarcely more than one percent of its initial value. It is presumably this abnormal depression of the CO peak which causes the apparent large increase in the C peak. Run No. 13 was made at a reduced pressure of CO, about one-fourth of the normal pressure of about 10^{-4} mm. Run No. 7 is shown as Fig. 5. (See Table II.)

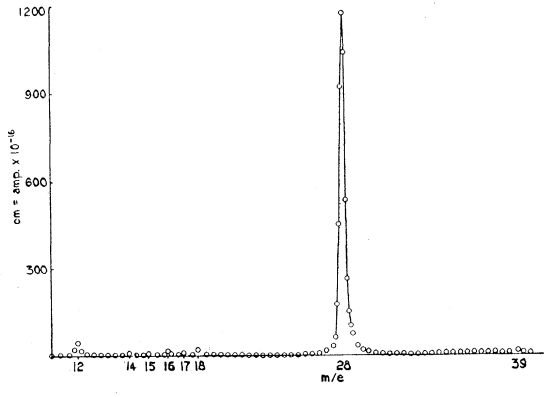

FIG. 5. Run No. 7. Carbon monoxide. 120 volt electrons. Height of CO peak = 1175 cm.

AMMONIA

The ammonia used was produced by heating a mixture of ammonium sulphate with a large excess of calcium oxide. Runs 21, 24 and 26 were made on a different sample which was further dried with KOH pellets, and show that the first sample was not satisfactorily dried (Fig. 6). It seems likely that the presence of

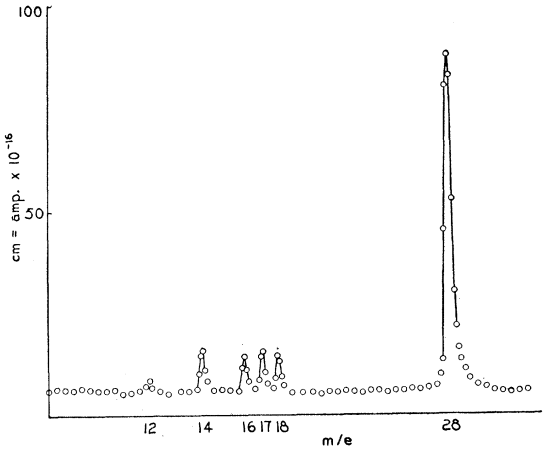

FIG. 6. Run No. 23. Ammonia. 81 volt electrons. Height of NH_3 peak = 9.7 cm.

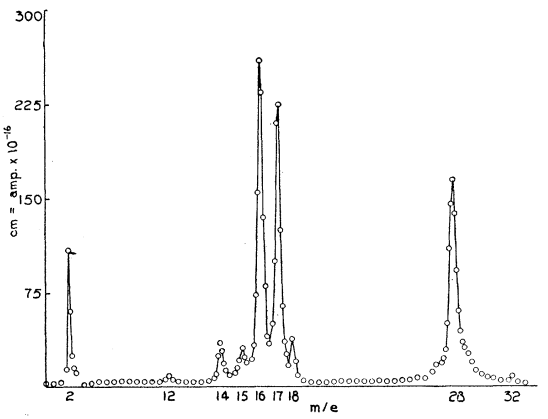

FIG. 7. Run No. 28. Hydrazine. 113 volt electrons. Height of NH_3 peak = 222 cm. The peak at 27 is not satisfactorily accounted for.

water vapor contributes to the high intensity observed for the N_2 peak, but this point will require further observation. It is to be noted that there is substantial equality between the NH_2 and NH_3 peaks, as has been reported previously by Bartlett.[2] (See Table III.)

HYDRAZINE

The sample of hydrazine used was kindly supplied by Professor Beckman of the chemistry department. It had been distilled three times over KOH and then stored for some months in contact with KOH so that its water content must have been far below that contributed by the walls of the apparatus.

Because the tube from which the vapor is released in the filament assembly is necessarily heated by radiation from the filaments, the hydrazine seems to be almost completely thermally decomposed. Thus the primary ion in this case is NH_3 and not N_2H_4. Run No. 28 is shown as Fig. 7. The entry t in the table means the peak was definitely present but of uncertain height. (See Table IV.)

TABLE IV. *Ion intensities observed for hydrazine bombarded with electrons of various energies. Intensities calculated to basis* $NH_3^+ = 100$.

Run	μa	ma	Volts	True NH_3	H_2	C	CH	N	NH	NH_2	NH_3	NH_4	CN	27	N_2	N_2H	N_2H_2	N_2H_3	N_2H_4
28	21	7.5	113	222	47	2.3	0.5	14	12	116	100	16	0.67	1	72	t	t	t	2.7
29	20	7	114	171	79	1.5	—	17	14	123	100	6.5	1	1.5	61	t	t	t	2.9
30	8	4	80	47	49	—	—	19	13	105	100	7.4	t	t	47	1.5	1	2	3
31	30	15	60	92	27	11	.6	6	5	102	100	141	—	—	84	t	t	t	3
32	15	10	40	40	57	5	—	2	4	81	100	20	—	t	57	2	—	—	—
33	.9	8	30	4	25	—	—	—	—	15	100	—	—	—	—	—	—	—	—
34	0.1	4.7	20	—	—	—													

Because of their great stability, nitrogen and carbon monoxide yield predominantly molecular ions. However, ammonia and hydrazine decompose readily to yield fractional ions, and can recombine in many different ways depending on collision probability.

Acknowledgment is made to Professor R. A. Millikan, under whose direction this work has been done, for his interest and helpful suggestions.

[2] James H. Bartlett, Jr., Phys. Rev. **33**, 169 (1929).